Batteries & Supercaps

Research Article
doi.org/10.1002/batt.202300550

Chemistry Europe
European Chemical Societies Publishing

www.batteries-supercaps.org

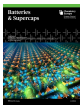

# *In situ* Electrolyte Design: Understanding the Prospects and Limitations of a High Capacity $Ca(BH_4)_2$ Anode for All Solid State Batteries

Yixin Chen,[a] Ryo Sakamoto,[b] Atsushi Inoishi,*[c] Shigeto Okada,[d] Hikari Sakaebe,[c] Ken Albrecht,[c] and Duncan H. Gregory*[e]

All-solid-state batteries have gained considerable attention due to their high safety and energy density. However, solid state electrolytes which contribute to the ionic conductivity component of a composite electrode, are not utilized during the electrode reaction and cannot directly contribute to capacity. This study focuses on decreasing the amount of electrolyte in the electrode by utilizing $Ca(BH_4)_2$ as an active electrode material. In this work, the charge-discharge properties of $Ca(BH_4)_2$ as an electrode material were determined for the first time. The lithiation of the $Ca(BH_4)_2$ anode creates $LiBH_4$ within the electrode mixture, providing new Li-ion conduction pathways within the composite electrode *in situ*. An electrode fabricated only from $Ca(BH_4)_2$ and acetylene black (AB) showed an initial capacity of 473 mAh $g^{-1}$ at 120 °C, which is comparable to the performance obtained from a composite electrode additionally containing electrolyte. Evidently, $Ca(BH_4)_2$ is a promising candidate negative electrode for increased energy density all-solid-state Li-ion batteries.

## Introduction

All-solid-state batteries (ASSBs) using non-flammable inorganic electrolytes instead of organic liquid electrolytes have attracted much attention as energy storage devices with high levels of safety and reliability.[1] ASSBs facilitate the bipolar configurations which provide Li-ion batteries (LIBs) with a route to higher volumetric energy density (achieved by stacking multiple electric cells in series within a single package).[2] The electrode compositions of commercial LIBs typically comprise more than 90% active material.[3,4] Active materials with high electronic conductivity render carbon additives unnecessary in a composite electrode.[5,6] However, in order to engender Li-ion and electron conductivity in an electrode in which the active material has both mediocre electronic and ionic transport properties, most reported electrode mixtures of ASSBs contain not only carbon additive but also solid electrolyte.[7,8] This approach will decrease the energy density of an ASSB because the added solid electrolyte and carbon components do not directly contribute to the capacity of the battery. Therefore, if the content of active material in a composite electrode mixture can be maximized without losing ionic conductivity and compromising contact with the electrolyte, then, the energy density of an ASSB could be dramatically improved. This would represent an encouraging new strategy to composite electrode design.

Several studies adopting this kind of strategy have been performed in cells with a variety of chemistries.[9–12] Among them, an ASSB design using an electrode layer without any conductive additives was reported by Nagao *et al* by blending $Li_2SO_4$ with transition metal oxides such as $Li_2RuO_3$[9] or $LiCoO_2$[11] as the active and electronically conducting material. $Li_2SO_4$ acts here so as to impart ionic conductivity to the active electrode material. Moreover, Sato *et al* reported an ASSB using $Mg(BH_4)_2$ and Acetylene black (AB) as a composite electrode without the necessity of the solid electrolyte as a component. The following conversion reaction occurred between $Li^+$ and $Mg(BH_4)_2$:[12]

$$Mg(BH_4)_2 + 2Li^+ + 2e^- \rightleftharpoons 2LiBH_4 + Mg \quad (1)$$

Importantly a solid electrolyte is not required as part of a $Mg(BH_4)_2$ composite due to the *in situ* formation of electrolyte in the borohydride electrode during lithiation. This thus negates

[a] Dr. Y. Chen
Interdisciplinary Graduate School of Engineering Sciences
Kyushu University
Kasuga-koen 6-1, Kasuga, Fukuoka, 816-8580, Japan

[b] Dr. R. Sakamoto
Office of Society Academia Collaboration for Innovation
Kyoto University
Funai Center, Nishikyo-ku, Kyoto 615-8530, Japan

[c] Dr. A. Inoishi, Prof. H. Sakaebe, Dr. K. Albrecht
Institute for Materials Chemistry and Engineering
Kyushu University
Kasuga-koen 6-1, Kasuga, Fukuoka, 816-8580, Japan
E-mail: inoishi@cm.kyushu-u.ac.jp

[d] Prof. S. Okada
Transdisciplinary Research and Education Centre for Green Technology
Kyushu University
Kasuga-koen 6-1, Kasuga, Fukuoka, 816-8580, Japan

[e] Prof. D. H. Gregory
WestCHEM, School of Chemistry
University of Glasgow
GlasgowG12 8QQ,United Kingdom
E-mail: Duncan.Gregory@glasgow.ac.uk

Supporting information for this article is available on the WWW under https://doi.org/10.1002/batt.202300550

the need to add $LiBH_4$ electrolyte to the anode in advance (as might be performed otherwise). Therefore, the active material content can be significantly increased from 40% to 70% and an improved actual capacity can be achieved.[12] The detailed solid process of *in situ* electrolyte formation is schematically illustrated in Fig. S1. $Mg(BH_4)_2$ operates at 0.8 V (vs. $Li/Li^+$), which is not a suitable redox potential for the negative electrode of a high voltage battery. An active material with a lower electrochemical potential is strongly desirable to perform the role of generating the electrolyte *in situ*. In this work, HT-$LiBH_4$ is also the target for the *in situ* electrolyte because of its favorable ductility and high ionic conductivity (of $10^{-3}$ S cm$^{-1}$ above the orthorhombic (LT) -hexagonal (HT) phase transition at 115 °C).[13,14] We therefore decided to focus on alternative borohydride-based salts (such as $Ca(BH_4)_2$, $KBH_4$, $NaBH_4$, etc.) as candidates for a suitable negative electrode material (that would generate $LiBH_4$ solid electrolyte *in situ*). Among them, $Ca(BH_4)_2$ is conspicuous in having a high theoretical capacity of 768 mAh g$^{-1}$. Moreover, $Ca(BH_4)_2$ has a lower electrochemical potential than that of $Mg(BH_4)_2$ given the presence of the Ca/$Ca^{2+}$ redox couple. The assumed reaction of $Ca(BH_4)_2$ would follow:

$$Ca(BH_4)_2 + 2Li^+ + 2e^- \rightleftharpoons 2LiBH_4 + Ca \quad (2)$$

theoretical capacity: 768 mAh g$^{-1}$

In this study, both $Ca(BH_4)_2$-AB and $Ca(BH_4)_2$-$LiBH_4$-AB composites were prepared as negative electrodes by ball-milling. This investigation represents the first report of $Ca(BH_4)_2$ as an active anode component in an ASSB. Our experiments reveal an impressive electrochemical performance and demonstrate the feasibility of $Ca(BH_4)_2$ towards *in situ* electrolyte formation. Furthermore, a better electrochemical performance was observed without using added $LiBH_4$ in the composite electrode, suggesting a more favorable interfacial contact can be achieved by utilizing an electrolyte formed *in situ*. Our approach has also enabled the reaction mechanism of the $Ca(BH_4)_2$ anode on (de)lithiation to be probed systematically.

## Results and Discussion

As detailed in the supporting information, the charge-discharge experiments were measured with a current density of 0.5 mA cm$^{-2}$ at 120 °C in an Ar atmosphere because $Ca(BH_4)_2$ is unstable in air condition. The all-solid-state half cells based on electrodes containing $LiBH_4$ electrolyte (sample **1**) show a large reversible capacity of 327 mAh g$^{-1}$ and exhibit a plateau at approximately 0.3 V vs. $Li/Li^+$ in the charge curve (i.e. during lithiation as $Ca(BH_4)_2$ is charged with Li) (Figure 1(a)). To the best of our knowledge, this is the first report of the use of $Ca(BH_4)_2$ as an anode material for an LIB. Compared to other reported $BH_4^-$ based active materials, a larger difference in the charge and discharge voltage was observed; i.e. 0.6 V for $Ca(BH_4)_2$ as compared with 0.1 V for $Mg(BH_4)_2$,[12] which indicates a higher resistance for the former in the respective charge-discharge process. Moreover, it is notable that the initial charge (lithiation) capacity of 424 mAh g$^{-1}$ is significantly lower than the theoretical capacity of 768 mAh g$^{-1}$ (as would be expected from equation 2). This indicates that other factors such as possible side reactions or impurities could inhibit the electrode reaction (a topic that we return to below). Importantly, and as anticipated, when compared to the redox potential of $Mg(BH_4)_2$ (*ca.* 0.8 V vs. $Li/Li^+$), $Ca(BH_4)_2$ exhibited a lower average voltage of close to 0.6 V vs. $Li/Li^+$. In principle, this wider potential range could be attractive for a prospective anode material for a high voltage battery.

By comparison, Figure 1(b) shows the charge-discharge profile of the composite electrode fabricated without added $LiBH_4$ electrolyte (sample **2**). This specimen exhibits an initial charge capacity of 470 mAh g$^{-1}$ and an initial reversible capacity of 417 mAh g$^{-1}$. Clearly, the electrode performance does not suffer notably from the omission of the electrolyte with no decrease in capacity observed. Hence appreciable ionic conductivity is imbued to the sample **2** by the electrolyte formed *in situ* during the lithiation process. Moreover, the actual capacity (i.e. capacity of the entire electrodes), which is shown in the upper x-axes of Figure 1 (a, b), for sample **2** (331 mAh g$^{-1}$) is much larger than the actual capacity of sample **1** (170 mAh g$^{-1}$) because of the increased content of active material in the electrode layer of the former.

A steep slope is apparent in the initial charging curve from 1.2 V to 0.5 V. A similar slope has also been observed in other ASSBs in which $LiBH_4$ has been used as the solid electrolyte. The distinctive feature is tentatively assigned to the formation of an SEI between the active materials and $LiBH_4$ in the electrode layer.[15,16] The content of $LiBH_4$ in sample **2** is less than that of sample **1**, therefore the capacity assigned to this slope for sample **2** is 53 mAh g$^{-1}$ which is smaller than the value of 77 mA h g$^{-1}$ for sample **1**. To investigate the origin of the plateau present at *ca.* 0.75 V in the 2$^{nd}$ lithiation curve, charge-discharge measurements were performed for sample **1** using voltage ranges of 0.2 V~1.4 V and 0.2 V~1.0 V (Fig. S2). A small plateau is clearly observable at 0.75 V in the 2$^{nd}$ lithiation curve. After changing the discharge cut-off voltage to 1.0 V, the plateau at 0.75 V disappeared in the 4$^{th}$ lithiation curve, indicating this plateau is associated with the reversible capacity of the slope above 1.0 V in the delithiation process. However, the higher capacity attributable to the slope above 1.0 V suggests this higher voltage feature has some relation to the plateau at 0.8 V. The cycling performance of sample **1** is shown in Figure 1(c). Most significantly, when compared to the performance of sample **2** shown in Figure 1(d), the cycling capability of sample **1** did not improve when electrolyte was added to the electrode mixture. After 25 cycles, the capacity decayed to *ca.* 190 mAh g$^{-1}$ which is considerably lower than that of sample **2** over an equivalent period (*ca.* 260 mAh g$^{-1}$). This result indicates that the interface between the active materials and the solid electrolyte in sample **2** is more intimate and stable as a result of the *in situ* formation of $LiBH_4$ than that achieved by ball-milling the respective borohydrides at the outset in sample **1**. The coulombic efficiency during cycling is also shown in Figure 1(c,d). Both electrodes reach high efficiency quickly and there is no significant difference between

Research Article
doi.org/10.1002/batt.202300550
Chemistry Europe
European Chemical Societies Publishing

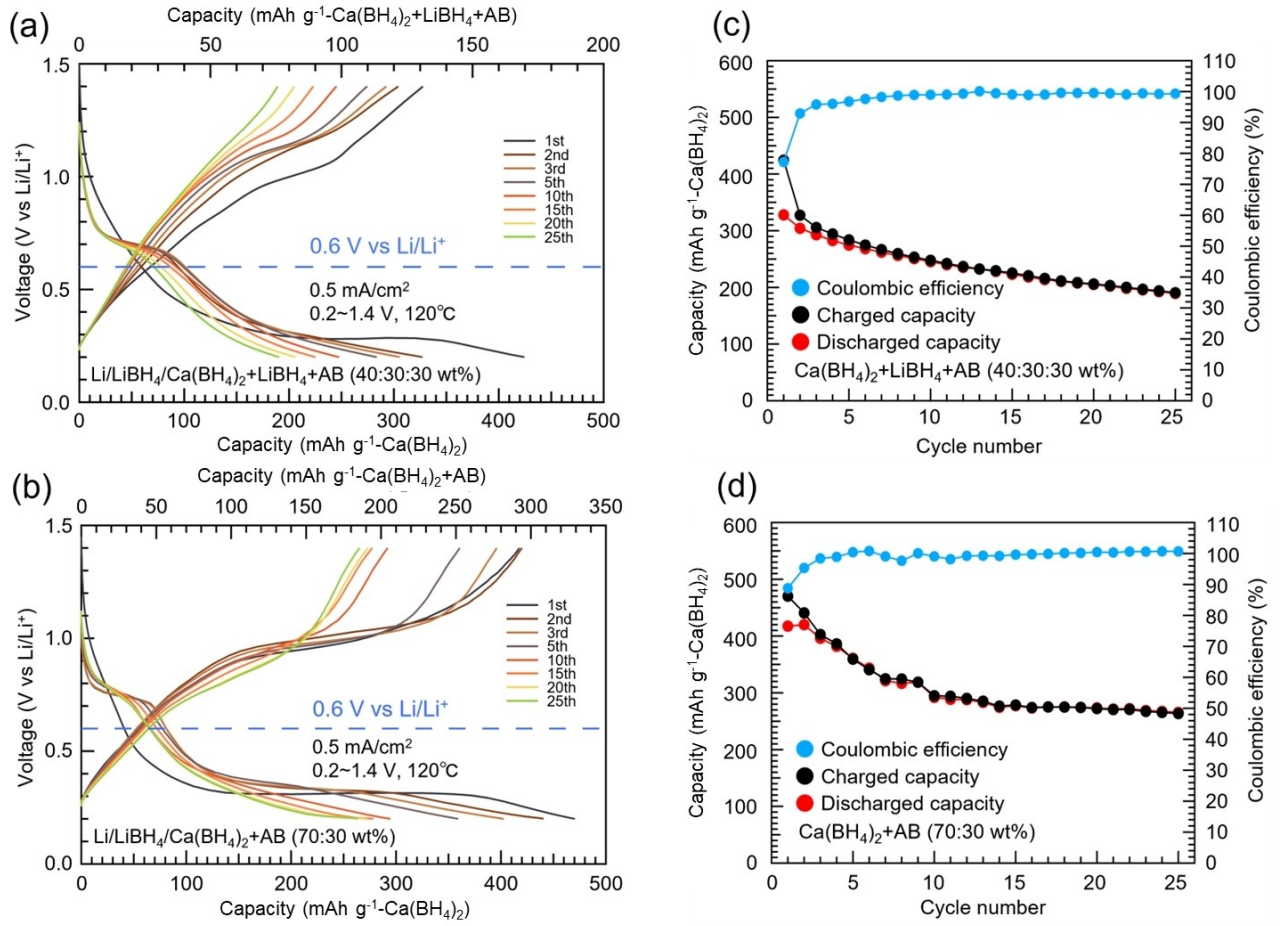


**Figure 1.** (a) Charge-discharge voltage profiles for sample **1** (initially 40:30:30 wt.% $Ca(BH_4)_2$:$LiBH_4$:AB); (b) charge-discharge voltage profiles of sample **2** (initially 70:30 wt.% $Ca(BH_4)_2$:AB); (c, d) cycling performance of sample **1** and sample **2**, respectively. The charge-discharge experiments were measured with a current density of 0.5 mA $cm^{-2}$ at 120 °C.

sample **1** and sample **2** over 25 cycles. It was consiedered that the relatively large volume expansion of $Ca(BH_4)_2$ (143%) may be the main reason of capacity degration along with cycling.

In order to investigate whether $LiBH_4$ is formed inside the electrode layer in the lithiation process, *ex-situ* EXAFS measurements were performed. The EXAFS spectra for sample **2** at various states of (dis)charge are illustrated in Figure 2. Spectra of pure $Ca(BH_4)_2$ and $LiBH_4$ are also shown for comparison. In the initial (pre-lithiated) state, the peak at 190.9 eV in the B K-edge EXAFS spectrum (Figure 2(a)) approximately matches with the maximum (190.9 eV) and edge positions in the equivalent spectrum for $Ca(BH_4)_2$ and very closely resembles previously reported spectra.[17] After lithiation (charging), the absorption edge energy shifts to 191.4 eV which is almost identical to the position of the edge in the equivalent EXAFS spectrum for $LiBH_4$.[18] This strongly indicates the formation of $LiBH_4$, which would result from the reaction between Li and $Ca(BH_4)_2$ as proposed in equation 2. After delithiation (discharging), the peak following the absorption edge is broadened with a maximum that shifts towards a lower photon energy. However, the position (and shape) of this peak in the spectrum of the sample in the delithiated state is not entirely consistent with the spectrum of $Ca(BH_4)_2$ (which once more is expected to show a maximum at 190.9 eV). This result from the delithiated state measurement indicates that the system is not completely reversible and that the materials do not entirely return to $Ca(BH_4)_2$. It was assumed that this result might be attributed to an irreversible side reaction that occurs during the charge-discharge process. From an examination of the Li K-edge EXAFS spectra (Figure 2(b)), the lithiated sample shows a well-defined peak at 59.3 eV which is entirely consistent with the Li K-edge spectrum for the reference sample of bulk $LiBH_4$. This peak does not appear in the Li K-edge spectrum for the sample in the delithiated state. These observations are therefore consistent with the formation of $LiBH_4$ during the lithiation process and its subsequent consumption during delithiation. The combined EXAFS results indicate that the *in situ* formation of ionically-conducting electrolyte is possible within the electrode containing the $Ca(BH_4)_2$ active material. It should also be noted that since both $LiBH_4$ and $Ca(BH_4)_2$ are moisture-sensitive, the peaks that appear at *ca.* 194 eV in the B K-edge spectra and at approximately 64 eV in the Li K-edge spectra can be considered

Research Article
doi.org/10.1002/batt.202300550
Chemistry Europe
European Chemical Societies Publishing

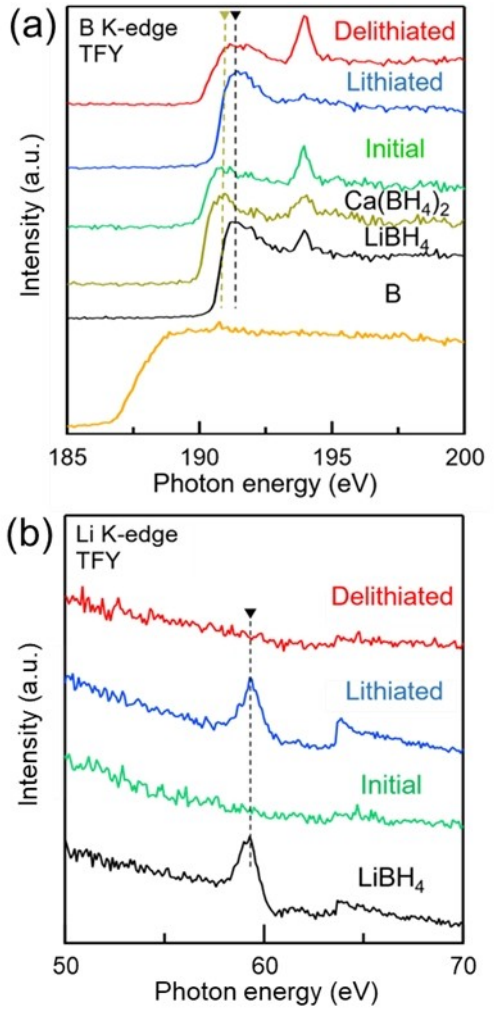


**Figure 2.** Ex-situ total fluorescence yield (TFY) mode EXAFS measurements of a $Ca(BH_4)_2$-AB composite electrode (**2**) in various charge states. (a) B K-edge spectra (black dashed line: $LiBH_4$, yellow dashed line: $Ca(BH_4)_2$) and (b) Li K-edge spectra (black dashed line: $LiBH_4$).

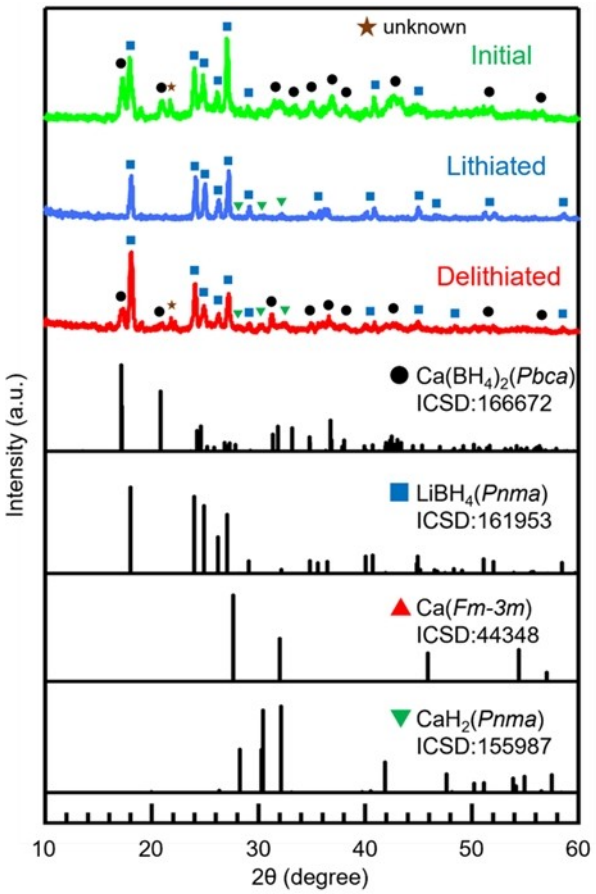


**Figure 3.** Comparison of ex-situ XRD patterns before and after the initial charge-discharge cycles of a $Ca(BH_4)_2$:AB (70:30 wt.%) composite electrode (**2**). Patterns generated from structures of possible products within the ICSD are shown for reference.

to be the result of the reaction of the borohydrides with air. By reference to previous studies, we can attribute the peaks that appear at *ca.* 194 eV in the B K-edge spectra to $B_2O_3$ or $LiBO_2$, and the peaks at approximately 64 eV in the Li K-edge spectra likely originate from $LiBO_2$ or $Li_2O$.[18,19]

To gain further understanding of the electrochemical reaction, *ex-situ* XRD measurements were performed at three different points of the charge-discharge cycling process; (i) the initial state (prior to cycling), (ii) the lithiatied state (after the first charge) and (iii) the de-lithiatied state (after the first discharge) (Figure 3). All of the samples used a double layer cell ($LiBH_4$ electrolyte layer/$Ca(BH_4)_2$ electrode layer) for XRD measurement. The initial sample (prior to cycling) contains $Ca(BH_4)_2$ as anticipated. The relatively broad peaks observed for the $Ca(BH_4)_2$ phase are expected from the ball milling process (causing both particle size reduction and likely microcrystalline strain).[20] For comparison, the experimental XRD pattern of the $Ca(BH_4)_2$ starting material can be found in Fig. S3. The diffractogram of this starting material shows that two phases of $Ca(BH_4)_2$ are initially present; the α-$Ca(BH_4)_2$ (orthorhombic) and β-$Ca(BH_4)_2$ (tetragonal) polymorphs. After ball milling, β-$Ca(BH_4)_2$ remains and α-$Ca(BH_4)_2$ is replaced by γ-$Ca(BH_4)_2$ (orthorhombic). Once Li reacts with $Ca(BH_4)_2$ to form the lithated electrode, there is no longer any evidence for $Ca(BH_4)_2$ peaks in the diffraction pattern suggesting that all of the calcium borohydride is consumed. However, no Ca metal peaks are observed in the lithiated electrode sample as would be expected from equation 2 and, in fact, peaks characteristic of $CaH_2$ appear and are especially noticeable in the 2θ range of 28°–32°. This result would suggest that either the electrode reaction is not that anticipated in equation 2 or that a side reaction occurs after lithiation is complete (and before the next delithiation cycle).

If the experimental electrode reaction does not follow the proposed process identified in equation 2, the reaction between Li and $Ca(BH_4)_2$ can result in the direct formation of $CaH_2$.

For example:

$$Ca(BH_4)_2 + Li \rightarrow LiBH_4 + CaH_2 + B + H_2 \quad (3)$$

$$2Ca(BH_4)_2 + 3Li \rightarrow 3LiBH_4 + 2CaH_2 + B \quad (4)$$

$$3Ca(BH_4)_2 + 5Li \rightarrow 5LiBH_4 + 2CaH_2 + Ca + B \quad (5)$$

All of these hypothetical reactions are accompanied with the formation of boron. Hence, the presence of free boron in the lithiated state would indicate the occurrence of one or more of these reactions during the de-lithiation process.

Solid state MAS NMR measurements were performed on sample **2** and compared to spectra measured for commercial $Ca(BH_4)_2$ and boron itself to establish whether boron is formed during the electrode reaction (Figure 4). The $^{11}B$ MAS NMR spectra taken across a range from 700 to −700 ppm are shown in Figure 4(a). The sharp peaks in the initial and lithiated states do not bear any resemblance to those from elemental boron. Considering Figure 4(b), which focuses on the resonances within a range of 10 to −50 ppm, commercial $Ca(BH_4)_2$ presents two peaks at chemical shifts of −30 and −33 ppm. These peaks originate from two different polymorphs of $Ca(BH_4)_2$. Minella *et al* reported that the signal at −30 ppm corresponds to the orthorhombic structure of the α-polymorph, whereas that at −33 ppm can be assigned to the tetragonal β-polymorph of the borohydride.[21] These findings are consistent with our XRD measurements which reveal that the as-received borohydride is a mixture of both α-$Ca(BH_4)_2$ and β-$Ca(BH_4)_2$. In the lithiated state, Li reacts with $Ca(BH_4)_2$ and the $^{11}B$ MAS NMR spectrum reveals a strong peak at −41 ppm which is almost identical to the reported spectrum for $LiBH_4$.[12] Strikingly, however, a sharp line at −0.1 ppm, which would be characteristic of boron, is not observed in the spectrum of the lithiated sample. These results suggest that B is not formed during the lithiation process. $Ca(BH_4)_2$ peaks emerge again in the delithiated state. The peak in this spectrum that can be observed at −41 ppm corresponds again to $LiBH_4$ and its appearance is somewhat inevitable given that $LiBH_4$ from the electrolyte layer will be present when the sample is prepared for NMR measurements.

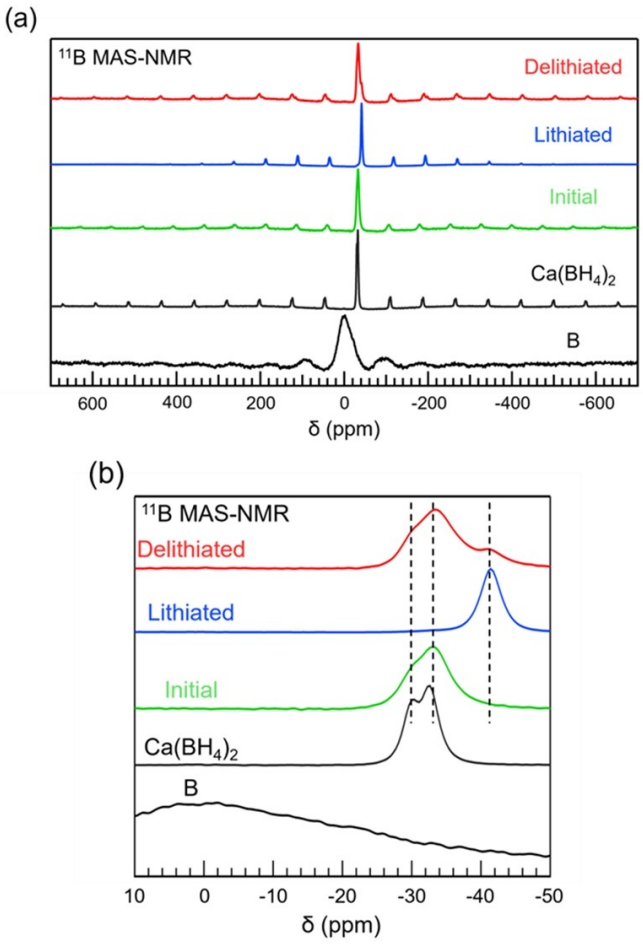


**Figure 4.** Solid state $^{11}B$ MAS NMR spectra taken from sample **2** in different charge states as compared to pure boron and $Ca(BH_4)_2$ showing: (a) spectra over the full spectral window and (b) expanded spectra from 10 to −50 ppm.

In order to probe the possibility of boron formation still further, *ex-situ* EXAFS (Figure 2(a)) at the B L-edge region was also performed. A peak which would be consistent with free elemental boron is not observed in any of the samples in the initial, lithiated or de-lithiated states, indicating free boron does not form during charge-discharge. This observation is thus consistent with the result of MAS NMR measurement. From the combined experimental evidence, it seems unlikely, therefore, that reactions which lead to B and $CaH_2$ (such as equations 3–5) occur on lithiation.

To examine the possible reasons behind the presence of $CaH_2$ in the cell, the lithiated electrode (sample **2**)was left to stand for 3 h at 120 °C in the Ar glove box prior to XRD measurement (Fig. S4). Evidently, the intensities of the $CaH_2$ peaks increase significantly after this time period (as compared with an electrode normally at rest for only ca. 1 minute at 120 °C after lithiation and before *ex-situ* characterisation). Therefore, we tentatively propose that $CaH_2$ continues to form from the reaction between Ca and $LiBH_4$ during the period of time following lithiation, given also that the cell is at a temperature of 120 °C. Rationally, there are other examples of $CaH_2$ formation when using $Ca(BH_4)_2$, for example, when $LiBH_4/CaBH_4$ composites were heat treated and when $Ca(BH_4)_2$/THF electrolyte was used with Ca metal electrodes, demonstrating the high reactivity of Ca metal.[22,23] Given that no diffraction peaks or $^{11}B$ resonances from any solid state boron-containing compounds are detected, it might be speculated that diborane ($B_2H_6$) gas, which is a typical thermal decomposition product of borohydrides, is formed and released, thus accounting for the apparent boron deficit.[23,24] The formation of $B_2H_6$ will be clarified by evolved gas analysis using mass spectroscopy in future studies. No new peak corresponding to compounds contained Li was observed in the Fig. S8 (XRD patterns of lithiated state rest for 3 h after lithiation process), indicating the amorphous structure of byproduct contained Li atom. However, it is difficult to identify the chemical formula.

Ca metal is not observed in the XRD patterns of samples taken in the lithiated state. This suggests that if Ca metal is formed during the lithiation process then the metal likely possesses a nanocrystalline or amorphous structure. When discharging the cell, $Ca(BH_4)_2$ peaks emerge again in the XRD patterns from delithiated samples, which is also consistent with the result of $^{11}B$ MAS NMR measurements. It is worthwhile

Research Article
doi.org/10.1002/batt.202300550
Chemistry Europe
European Chemical Societies Publishing

mentioning, however, that the $CaH_2$ peaks remain even after delithiation, indicating that the reaction between Ca and $LiBH_4$, in the lithiated state, is irreversible and so it is not possible for the lithiated products to then reform $Ca(BH_4)_2$ completely. As is clear from the diffraction patterns in Figure 3, peaks originating from $LiBH_4$ were observed in all samples irrespective of (dis)charge state, but as noted above, from the nature of the XRD samples taken from the cells, it is not possible to distinguish whether the $LiBH_4$ is present in the electrode layer (having formed from $Ca(BH_4)_2$ during lithiation) or it originates from the electrolyte layer itself.

Given the apparent absence of Ca in lithiated materials by XRD, further clarification was sought to test the premise that Ca is a reaction product of Li and $Ca(BH_4)_2$ as postulated in equation (2). *Ex-situ* XPS measurements of the initial, lithiated and delithiated states of sample **2** were performed. The Ca 2p XPS spectra are displayed in Figure 5 (The split in the binding energy between $2p_{1/2}$ and $2p_{3/2}$ is 3.5 eV. The FWHM of the fitted doublets of different states are 2.26 eV (Initial and lithiated state) and 1.95 eV (delithiated state). The height ration between $2p_{1/2}$ and $2p3_{/2}$ is 0.51:1 ($2p_{1/2}$:$2p_{3/2}$)). In the initial state (corresponding to $Ca(BH_4)_2$), two characteristic peaks are observed at 351 eV and 347.5 eV, which correspond to the $2p_{1/2}$ and $2p_{3/2}$ spin-orbit doublets. After lithiation, the Ca 2p peaks are shifted to lower binding energy, appearing at 349.8 eV and 346.3 eV respectively. These latter peak positions are consistent with the XPS spectrum from metallic Ca(0),[25] indicating that formation of Ca metal does indeed occur during the lithiation process. In the delithiated state, the characteristic peaks Ca 2p peaks return to the higher binding energies characteristic of Ca(II) in $Ca(BH_4)_2$. As indicated by the *ex-situ* EXAFS measurements, the lithiated products do not return entirely to $Ca(BH_4)_2$ due to the consumption of Ca to form $CaH_2$ (on reaction with $LiBH_4$).

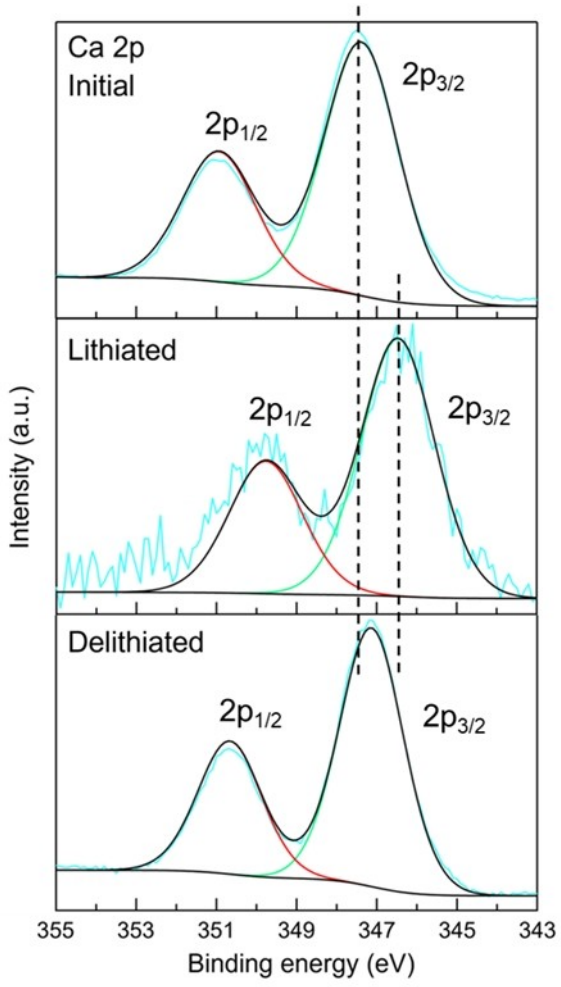


**Figure 5.** *Ex-situ* Ca 2p XPS measurement of a $Ca(BH_4)_2$-AB composite electrode in various charge states.

The proposed reaction mechanisms at the $Ca(BH_4)_2$ electrode might be summarized as below:

**(I) Lithiation process:**

$Li^+$ reacts with $Ca(BH_4)_2$ to form Ca metal and $LiBH_4$. according to eq. (2).

**(II) Period between charge and discharge:**

Active Ca metal reacts with $LiBH_4$ to form $CaH_2$ impurity irreversibly. (Boron-containing by-products are also formed; most likely gaseous $B_2H_6$)

**(III) Delithiation process:**

Remaining Ca metal reacts with $LiBH_4$ to form $Ca(BH_4)_2$.

Given the irreversible $CaH_2$ formation between charge and discharge, a fraction of the lithiated product ($LiBH_4$) does not return reversibly to $Ca(BH_4)_2$ and capacity is lost in the reverse reaction:

$$2LiBH_4 + (1\text{-}x)\ Ca \rightarrow (1\text{-}x)\ Ca(BH_4)_2 + xLiBH_4 + (2\text{-}x)Li^+ + (2\text{-}x)e^- \quad (6)$$

It is interesting to note that in the equivalent $Mg(BH_4)_2$/Li system no impurity such as $MgH_2$ was detected (by XRD or otherwise).[12] Given the possibility of metal hydrides acting as negative electrodes, we sought to consider the influence of $CaH_2$ as a possible active material and its contribution to the total capacity. To investigate this hypothesis we constructed an all-solid-state cell using $CaH_2$ as the active material under charge/discharge conditions employing a current density of 0.05 mA $cm^{-2}$ and an operating temperature of 120 °C. From the charge-discharge curves of $CaH_2$ (Fig. S5), it can be seen that a reversible capacity of only 16 mAh $g^{-1}$ was obtained. These observations reinforce the premise that $CaH_2$ does not contribute meaningfully to the capacity of the $Ca(BH_4)_2$ electrode.

However, in order to validate whether the performance could be affected by an increased proportion of $CaH_2$ within the *composite* borohydride electrode (**2**), we performed a series of galvanostatic intermittent titration test (GITT) measurements. As

Research Article
doi.org/10.1002/batt.202300550
Chemistry Europe
European Chemical Societies Publishing

shown in Fig. S6, we included a "rest period" of 6 h after every constant current charge process. With the exception of a slightly higher polarization, the performance of this battery was not dramatically influenced by the increased amount of $CaH_2$ contained in the electrode layer. These results suggest that the amount of $CaH_2$ formed in the cells with the electrode composition of **2** is not appreciable enough to impede the active material $Ca(BH_4)_2$ substantially. Further, the results indicate that polarization effects are not significant in these cells (despite the consideration that $CaH_2$ has poor electronic conductivity with a band gap of 5.84 eV).[26] It is nevertheless worth noting that the Coulombic efficiency of this battery (ie. rested for 6 h) is only 85%, which is lower than the 90% efficiency achieved for sample **2** (which is at rest for only 1 min between discharging and charging). Hence there is a direct link between the rest time and Coulombic efficiency (reversibility) as a progressively greater proportion of lithiated products (i.e. Ca) are consumed during the rest period.

For the purpose of maximizing the energy density of an ASSB, there are clear advantages in using as thick an electrode layer as possible. Therefore it is useful to investigate whether the electrolyte formed *in situ* would extend to the entire electrode layer if the thickness of $Ca(BH_4)_2$/AB is increased (and conversely, therefore, whether the concept breaks down at a maximum thickness level). The charge-discharge curves and cycle performance of a half-cell using a 290 μm-thick electrode layer (produced by an electrode mixture of 20 mg) are shown in Figure 6(a). This cell exhibited an initial reversible capacity of 373 mAh g$^{-1}$ and a charge capacity of 425 mAh g$^{-1}$ that did not decay dramatically when compared to sample **2** (which utilized 6 mg of electrode mixture giving a thickness of 87 μm and an initial reversible capacity of 417 mAh g$^{-1}$). The Such a capacity retention with increased electrode thickness is not universally observed in "in situ" LIB solid electrolyte systems. For example, $MgCl_2$ exhibits a significant decrease in the initial lithiated capacity when the thickness of the electrode layer is increased.[27] Comparing these results demonstrates that the ionic conductivity of the *in situ* solid electrolyte plays an essential role in the charge-discharge performance of the composite electrode (viz. LiCl: $\sigma = 5.9\times10^{-5}$ S cm$^{-1}$ at 120 °C[27] vs. $LiBH_4$: $\sigma \approx 10^{-3}$ S cm$^{-1}$ at 120 °C). Nevertheless, when comparing the extended cycling performance of the thicker electrode to the original cell of sample **2** (Fig. S7), then the performance was notably inferior; the charge capacity decreased to 119 mAh g$^{-1}$ after 25 cycles (*cf.* sample **2** with a capacity of 265 mAh g$^{-1}$ after 25 cycles). The poorer cycle performance and reduction in capacity is likely to be caused by the higher internal resistance of the thicker electrode layer and the faster degradation rate of the Li counter electrode due to the higher loading of active materials.[28] Encouragingly, when the amount of electrode mixture is increased still further to 30 mg, giving a calculated electrode thickness of 435 μm, the cell still shows a high initial charge capacity of 418 mA h g$^{-1}$ and continues to act reversibly (Figure 6(b)). In practical terms, the 30 mg electrode is much thicker than the vast majority of those reported in ASSBs,[29–31] and the results imply that the electrode reaction

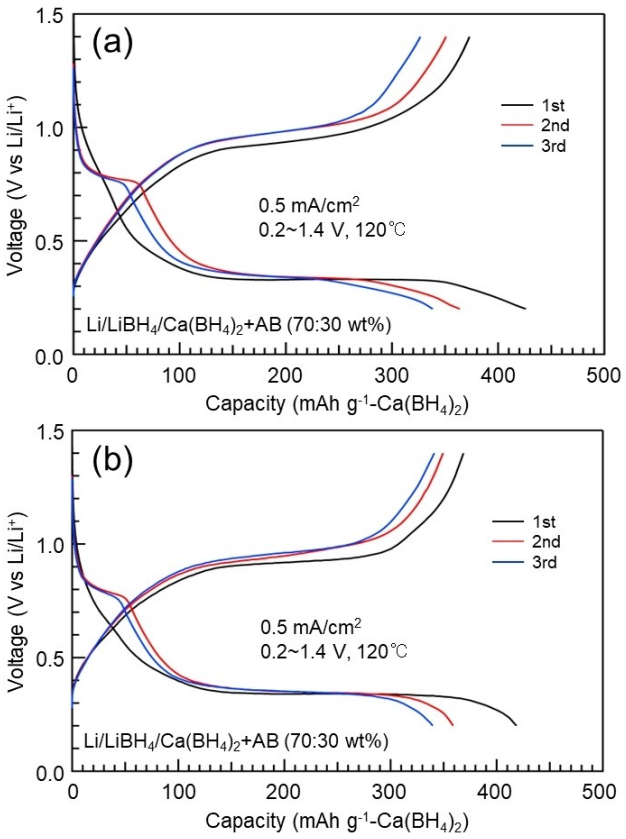


**Figure 6.** Charge-discharge voltage profiles of a $Ca(BH_4)_2$-AB composite electrode in which the electrode thickness was increased to: (a) 290 μm (electrode mixture of 20 mg) and (b) 435 μm (electrode mixture of 30 mg).

successfully proceeds via the *in situ* formation of electrolyte even with an electrode layer approaching $^1/_2$ mm.

The extent of the electrochemical reaction across the thicker (290 μm) electrode layer (produced by an electrode mixture of 20 mg) was probed *via ex-situ* EXAFS measurements performed on lithiated samples (Fig. S8). The B K-edge EXAFS spectra (Fig. S8(a)) showed evidence of a peak at 191.4 eV, which is in close agreement with the equivalent spectrum of the original thinner lithiated electrode (using an electrode mixture of 6 mg) and once again matches well to the $LiBH_4$ reference material. Furthermore, comparison of the Li K-edge EXAFS spectra (as shown in Fig. S8(b)) shows that the peak at 59.3 eV in the lithiated thick electrode sample (electrode mixture of 20 mg) is in a virtually identical position to the Li K-edge EXAFS spectra of both the $LiBH_4$ bulk reference and the original lithiated thin electrode sample (produced from an electrode mixture of 6 mg). The EXAFS results thus strongly indicate that $LiBH_4$ is formed *in situ* across the entire electrode layer, even when increasing the thickness by more than a factor of 5.

## Conclusions

$Ca(BH_4)_2$ has been utilized as a negative electrode material in a rechargeable LIB for the first time. The borohydride electrodes

show a large charge capacity of 470 mAh g$^{-1}$ despite evident polarization effects. The results indicate that $Ca(BH_4)_2$ should be more suitable than $Mg(BH_4)_2$ for the fabrication of high voltage LIB given its lower redox potential of 0.6 V vs. Li/Li$^+$. Moreover, importantly, because of the *in situ* formation of $LiBH_4$ during the lithiation process, no solid electrolyte component is required in the fabricated composite electrode (i.e. only the active material and activated carbon are required) and the actual capacity can be significantly improved from 170 to 331 mAh g$^{-1}$. Compared to established approaches in which the electrolyte is combined with the active electrode material by ball-milling, it was considered that an electrolyte formed *in situ* provides superior interfacial contact between the active electrode materials and the solid electrolyte. Closer probing of the charge/discharge process reveals that $CaH_2$ impurity (itself only partially reversible and contributing close to negligible capacity to the battery) is formed during cycling and that this appears to occur principally at the time *between* charge and discharge; minimizing these "rest periods" therefore reduces the scale of impurity formation. Preliminary experiments suggest that the energy density of these LIBs could be increased further without compromising the *in situ* electrolyte formation concept. For example, a $Ca(BH_4)_2$ battery with a thicker electrode (20 mg≡290 μm thickness) also cycled reversibly and showed comparable capacity to a battery with a thinner electrode (6 mg≡87 μm) in initial cycle. Among other technical considerations, the operating temperature (120 °C) is a stumbling block for practical utilization. Therefore decreasing the operating temperature through materials design is an important subject of our future research. Nevertheless, more broadly, with a degree of design optimization, the unique concept of *in situ* electrolyte formation, which not only increases the active material content, but also provides intimate interfacial contact, promises to be an important factor in the development of high-capacity negative electrode materials for ASSBs.

## Supporting Information

Experimental details and further figures are provided. The authors have also cited additional references within the Supporting Information.

## Acknowledgements

This work was in part supported by JSPS KAKENHI Grant Number JP20H05297, JP22H04621 (Grant-in-Aid for Scientific Research on Innovative Areas "Interface IONICS"), JST Grant Number JPMJFS2132 (the establishment of university fellowships towards the creation of science technology innovation), Grant-in-Aid for "2019 Initiative for Realizing Diversity in the Research Environment" through the "Diversity and Super Global Training Program for Female and Young Faculty (SENTAN-Q)", Kyushu University from MEXT and "Dynamic Alliance for Open Innovation Bridging Human, Environment and Materials" from the MEXT. D. H. G. thanks Kyushu University for support under the Progress 100 program. The experiments using synchrotron radiation were performed at the beamline BL12 of the SAGA Light Source (Proposal No. 2204025F and 2012137R).

## Conflict of Interests

The authors declare no conflict of interest.

## Data Availability Statement

The data that support the findings of this study are available from the corresponding author upon reasonable request.

**Keywords:** All-solid-state battery · *in situ* electrolyte · negative electrode · $Ca(BH_4)_2$

[1] J. Janek, W. G. Zeier, *Nat. Energy* **2016**, *1*, 16141.
[2] Y. Gambe, Y. Sun, I. Honma, *Sci. Rep.* **2015**, *5*, DOI 10.1038/srep08869.
[3] M. Beak, S. Park, S. Kim, J. Park, S. Jeong, B. Thirumalraj, G. Jeong, T. Kim, K. Kwon, *J. Alloys Compd.* **2021**, *873*, DOI 10.1016/J.JALLCOM.2021.159808.
[4] O. Chaouachi, J. M. Réty, S. Génies, M. Chandesris, Y. Bultel, *Electrochim. Acta* **2021**, *366*, DOI 10.1016/J.ELECTACTA.2020.137428.
[5] F. Strauss, T. Bartsch, L. De Biasi, A.-Y. Kim, J. Rgen Janek, P. Hartmann, T. Brezesinski, *ACS Energy Lett.* **2018**, *3*, 992.
[6] T. Takeuchi, H. Kageyama, K. Nakanishi, T. Ohta, A. Sakuda, H. Sakaebe, H. Kobayashi, K. Tatsumi, Z. Ogumi, *ECS Electrochem. Lett.* **2014**, *3*, A31.
[7] M. Nagao, A. Hayashi, M. Tatsumisago, *Electrochim. Acta* **2011**, *56*, 6055.
[8] K. Kawahito, L. Zeng, T. Ichikawa, H. Miyaoka, Y. Kojima, *Mater. Trans.* **2016**, *57*, 755.
[9] K. Nagao, Y. Nagata, A. Sakuda, A. Hayashi, M. Deguchi, C. Hotehama, H. Tsukasaki, S. Mori, Y. Orikasa, K. Yamamoto, Y. Uchimoto, M. Tatsumisago, *Sci. Adv.* **2020**, *6*, 1.
[10] K. Nagao, A. Sakuda, A. Hayashi, H. Tsukasaki, S. Mori, M. Tatsumisago, *Adv. Mater. Interfaces* **2019**, *6*, 2.
[11] K. Nagao, Y. Nagata, A. Sakuda, A. Hayashi, M. Tatsumisago, *MRS Adv.* **2018**, *3*, 1319.
[12] H. Sato, R. Sakamoto, H. Minami, H. Izumi, K. Ideta, A. Inoishi, S. Okada, *Chem. Commun.* **2021**, *57*, 2605.
[13] M. Matsuo, Y. Nakamori, S. I. Orimo, H. Maekawa, H. Takamura, *Appl. Phys. Lett.* **2007**, *91*, 2.
[14] Y. Filinchuk, D. Chernyshov, R. Cerny, *J. Phys. Chem. C* **2008**, *112*, 10579.
[15] L. Zeng, K. Kawahito, S. Ikeda, T. Ichikawa, H. Miyaoka, Y. Kojima, *Chem. Commun.* **2015**, *51*, 9773.
[16] A. H. Dao, N. Berti, P. López-Aranguren, J. Zhang, F. Cuevas, C. Jordy, M. Latroche, *J. Power Sources* **2018**, *397*, 143.
[17] C. J. Sahle, C. Sternemann, C. Giacobbe, Y. Yan, C. Weis, M. Harder, Y. Forov, G. Spiekermann, M. Tolan, M. Krisch, A. Remhof, *Phys. Chem. Chem. Phys.* **2016**, *18*, 19866.
[18] P. S. Miedema, P. Ngene, A. M. J. Van Der Eerden, T. C. Weng, D. Nordlund, D. Sokaras, R. Alonso-Mori, A. Juhin, P. E. De Jongh, F. M. F. De Groot, *Phys. Chem. Chem. Phys.* **2012**, *14*, 5581.
[19] R. Qiao, Y. De Chuang, S. Yan, W. Yang, *PLoS One* **2012**, *7*, e49182.
[20] T. D. Shen, W. Q. Ge, K. Y. Wang, M. X. Quan, J. T. Wang, W. D. Wei, C. C. Koch, *Nanostruct. Mater.* **1996**, *7*, 393.
[21] C. Bonatto Minella, S. Garroni, C. Pistidda, R. Gosalawit-Utke, G. Barkhordarian, C. Rongeat, I. Lindemann, O. Gutfleisch, T. R. Jensen, Y. Cerenius, J. Christensen, M. D. Baró, R. Bormann, T. Klassen, M. Dornheim, *J. Phys. Chem. C* **2011**, *115*, 2497.
[22] D. Wang, X. Gao, Y. Chen, L. Jin, C. Kuss, P. G. Bruce, *Nat. Mater.* **2018**, *17*, 16.
[23] D. Sveinbjörnsson, D. Blanchard, J. S. G. Myrdal, R. Younesi, R. Viskinde, M. D. Riktor, P. Norby, T. Vegge, *J. Solid State Chem.* **2014**, *211*, 81.
[24] D. Blanchard, Q. Shi, C. B. Boothroyd, T. Vegge, *J. Phys. Chem. C* **2009**, *113*, 14059.
[25] C. J. Powell, *J. Electron Spectrosc. Relat. Phenom.* **2012**, *185*, 1.

[26] J. H. Weaver, M. Gupta, D. T. Peterson, *Solid State Commun.* **1984**, *51*, 805.
[27] A. Inoishi, M. Suyama, E. Kobayashi, S. Okada, H. Sakaebe, *Batteries & Supercaps* **2023**, DOI 10.1002/batt.202300187.
[28] J. Park, C. Jeon, W. Kim, S. J. Bong, S. Jeong, H. J. Kim, *J. Power Sources* **2021**, *482*, DOI 10.1016/J.JPOWSOUR.2020.228948.
[29] R. Xu, J. Yue, S. Liu, J. Tu, F. Han, P. Liu, C. Wang, *ACS Energy Lett.* **2019**, *4*, 1073.
[30] W. Zaïdi, Y. Oumellal, J. P. Bonnet, J. Zhang, F. Cuevas, M. Latroche, J. L. Bobet, L. Aymard, *J. Power Sources* **2011**, *196*, 2854.
[31] J. Auvergniot, A. Cassel, J. B. Ledeuil, V. Viallet, V. Seznec, R. Dedryvère, *Chem. Mater.* **2017**, *29*, 3883.

Manuscript received: November 24, 2023
Revised manuscript received: January 17, 2024
Accepted manuscript online: January 17, 2024
Version of record online: February 2, 2024